FUDMA Journal of Sciences (FJS)
ISSN online: 2616-1370
ISSN print: 2645 - 2944
Vol. 10 No. 23, December, 2026, pp 29 – 40
DOI: https://doi.org/10.33003/fjs-2026-1023-6316

Development and Performance Evaluation of a Timer-Controlled Solar- Powered Drip Irrigation System for Smallholder Farmers

[*1]Donatus Okwudiri Igbojionu. [1]Valentine Ngozi Ekejiuba, [2]Juliet Nnennaya Igbojionu

[1]Department of Agricultural & Bio-environmental Engineering, Federal College of Land Resources Technology, Owerri, Imo State, Nigeria.
[2]Department of Soil Science and Land Resources Management, Federal College of Land Resources Technology, Owerri, Imo State, Nigeria.

*Corresponding authors' email: igbojionudonatus@gmail.com

Received: 27 Sept. 2026
Accepted: 06 Nov. 2026
Published: 10 Nov. 2026

ABSTRACT
This study developed and evaluated a timer-controlled solar-powered drip irrigation system for smallholder farming. The system used an ESP32 microcontroller and DS3231 real-time clock to schedule irrigation across a 70-day cucumber growth cycle. Hydraulic performance was assessed using coefficient of uniformity (CU), emission uniformity (EU), coefficient of variation (CV) and flow variation (FV). Timer performance was evaluated across four growth stages by comparing actual and programmed irrigation durations. The power subsystem comprised a 50 W PV module, a 10 A/12 V PWM charge controller and a 12 V, 70 Ah lead-acid battery. It was estimated to generate 168.75 Wh/day against an adjusted demand of 100.9 Wh/day, providing about 4.16 days of autonomy at 50% depth of discharge. The pump drew 83.2 W (≈6.93 A at 12 V), and PV output was projected to meet demand at 2.69 peak sun hours/day, below which the battery supplied the deficit. The system achieved CU and EU of 96.74% and 95%, indicating high water-distribution uniformity. CV was 3.96% and FV was 14.63%. Timer errors ranged from −0.94% to +2.68%, with the largest error during the 41-minute mid-season schedule. Analysis of variance showed significant differences in timer error among growth stages ($F = 80.86$, $p < 0.001$). These findings demonstrate favourable hydraulic uniformity, timing performance and nominal power-subsystem adequacy. However, crop-yield improvement, water savings and long-term solar reliability were not independently established. Further field evaluation, including solar-energy performance, irrigation-water application and crop response, is recommended before wider deployment.

Keywords: Solar-Powered Drip Irrigation; Timer-Based Control; ESP32-DS3231; Hydraulic Uniformity; Emission Uniformity; Irrigation Scheduling, Timer-Based Irrigation, Solar Powered Irrigation, Drip Irrigation, Smallholder Farmers, Automation.

INTRODUCTION

In southeastern Nigeria, particularly Owerri, Imo State, smallholder vegetable and staple crop production is predominantly rain-fed, rendering farmers highly vulnerable to climate variability, erratic rainfall distribution, and prolonged dry seasons (Olayide et al., 2016). Recent climatic data for Owerri show an average annual rainfall of 2,200–2,500 mm concentrated between March and November, leaving a distinct 4–5-month dry season during which farming activities are largely abandoned, exacerbating seasonal food scarcity and income loss (NIMET, 2023). Irrigation is a proven strategy to de-risk rain-fed agriculture, enhance food security (Adeyolanu & Okelola, 2024), and support the transition from subsistence to commercial farming (Amaechina & Eboh, 2013). Among available methods, drip irrigation offers high water-use efficiency (90–95%) by delivering water directly to the rhizosphere and minimising evapotranspiration, runoff, weed proliferation, and nutrient leaching (Erdem et al., 2010; FAO, 2021). This aligns with localised assessments, such as those in the Zobe Irrigation Area of Katsina State, which recommend drip irrigation as an effective technique for enhancing water-use efficiency (Bichi & Abdulyakin, 2025), and with field evaluations in tropical agroecological zones showing that calibrated drip irrigation can optimise water productivity and improve yields of high-value crops such as cucumber (Igbojionu et al., 2026). However, conventional drip systems in Nigeria rely on grid electricity, which is unreliable in rural Owerri communities, or petrol-powered pumps, whose operating costs have risen sharply following fuel subsidy removal, placing them beyond the reach of many resource-poor farmers.

Solar-powered irrigation has emerged as a sustainable, off-grid alternative, using photovoltaic (PV) energy to drive water pumps with zero fuel cost and minimal carbon footprint (IRENA, 2023). The performance of such a system depends on the relationship between PV generation, pump performance, water delivery, and energy storage. PV output varies with solar irradiance, and the pump must be matched to the available power, total head, and required flow rate; water delivery through drip laterals then depends on emitter discharge and operating pressure. Energy storage, such as a battery, or water storage in a tank can buffer temporal mismatches between PV generation and irrigation demand. A solar-powered system is therefore appropriate for Owerri because it can operate off-grid in rural communities where electricity supply is unreliable, while the proposed design addresses electricity-supply limitations by using PV energy to drive the pump and a timer controller to manage pump operation and irrigation duration. Nevertheless, solar irrigation has been piloted mainly in Northern Nigeria, and its adoption in the humid southeast remains limited. Moreover,

most existing solar systems operate continuously when solar irradiance is available, without intelligent control; such uncontrolled pumping can lead to over-irrigation, which is wasteful and agronomically detrimental. Research has established that over-irrigation can suppress beneficial soil enzymes, thereby disrupting nitrogen cycling and nutrient availability (Kuzyakov et al., 2019; Li et al., 2023; Sherkuziyeva et al., 2025).

It is important to distinguish irrigation automation from irrigation optimisation. A timer-controlled system can improve scheduling consistency, but it does not necessarily ensure that the amount of water applied matches actual crop-water requirements. Optimisation requires consideration of crop water requirement (CWR), reference evapotranspiration (ETo), soil-water availability, emitter discharge, and irrigation duration. In practice, CWR can be estimated from ETo and crop coefficients, soil-water availability influences irrigation interval, and emitter discharge and the number of emitters determine the application rate and required irrigation duration. Timer-controlled automation presents a low-cost and robust alternative to expensive soil-moisture-based IoT systems that require internet connectivity and high technical know-how, which are unsuitable for rural Owerri. A timer-based controller can enable automated scheduling based on CWR and ETo, and previous studies in similar agro-ecologies have suggested that timer-automated drip irrigation can save water and improve yields compared with manual irrigation (Yuan et al., 2004; Pavithra et al., 2018; FAO, 2022; IRENA, 2023). However, there is a paucity of empirical data on locally designed, low-cost timer-based drip systems adapted to the plot size (0.1–0.5 ha) and socio-economic context of Owerri smallholders.

The research gap therefore concerns the limited empirical evidence on low-cost, offline timer-controlled solar-powered drip irrigation adapted to smallholder conditions in Owerri. Existing automated drip systems are often based on soil-moisture sensing and IoT connectivity, which are costly and technically demanding, while existing solar-powered systems often operate without controlled scheduling. The principal contribution of the proposed system is not a new optimisation algorithm or a soil-moisture feedback controller, but the integration of low-cost offline timer control with a solar-powered drip system, crop-stage scheduling for cucumber, and empirical evaluation of hydraulic uniformity and irrigation-timing performance. This distinguishes the study from previous work that has focused separately on solar pumping, drip hydraulic performance, or advanced automated irrigation.

This study aimed to develop and evaluate the hydraulic uniformity and irrigation-timing performance of a timer-controlled solar-powered drip irrigation system programmed for the growth stages of cucumber cultivation.

MATERIALS AND METHODS

Description of Study Area

The study was conducted at students' research and demonstration farm of the Federal College of Land Resources Technology, Owerri located at Oforola, Nigeria (Figure 1). The study area lies between latitude $5^{0}24^{1}$N and longitude $6^{0}54^{1}$E and occupies an elevation of 60m above mean sea level.

The annual rainfall ranges from 2000 – 2500mm while the temperature ranges from 27^{0} – 31^{0}C. The relative humidity varies from 80 – 85% during the rainy season which runs from April – October and 63 – 70% during the dry season spanning November to March. The soil is predominantly sandy clay loam with dry bulk density of 1.67 g/cm3.

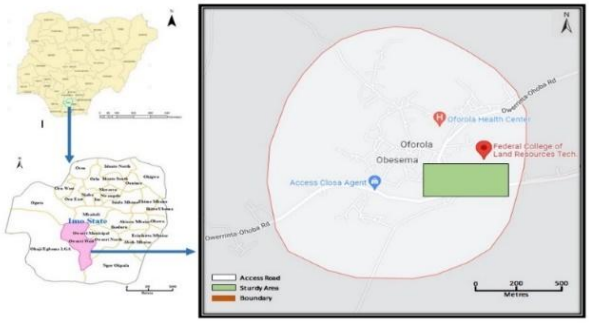


Figure 1: Map of Imo State Showing the Study Area

Data Generation

Irrigation Scheduling

The timer was programmed around four cucumber growth stages over a 70-day period. The stage crop water requirement was calculated as:

$$ET_{cstage} = ET_o \times K_{cstage} \quad (1)$$

Where:

ET_{cstage} = stage crop water requirement (mm/day)

ET_o = reference crop evapotranspiration (mm/day) = 5.0 mm/day

K_{cstage} = growth stage crop coefficient (dimensionless) - 0.45, 0.70, 0.90, 0.75 for cucumber stage

Growth stage gross irrigation requirement was computed as:

$$GIR_{stage} = \left(ET_{cstage} \times P_{wstage}\right)/E_a \quad (2)$$

Where:

GIR_{stage} = stage gross water requirement (mm/day)

Pw = percentage wetted area (decimal) - 0.5, 0.7, 0.8, 0.8 for cucumber stages

Ea = application efficiency(decimal) = 0.90

Daily volume of water applied was computed as:

$$V_d = GIR_d \times A \quad (3)$$

$$W_p = GIR_d \times S_r \times S_p \quad (4)$$

Where:

V_d =daily volume of water applied (L/day)

GIR_d = daily gross irrigation requirement (mm/day)

A = area of plot (m^2) =$10m^2$

Wp = water requirement per plant (L/plant/day)

Sr = row spacing (m) = 1.0 m

Sp = plant spacing (m) = 0.30m

Time to apply irrigation water at each growth stage was calculated as:

$T_{stage} = W_{pstage}/q$ (5)

Where:

Wp = daily stage water applied (L/day)
Q = emitter discharge = 2 L/h

Table 1: Derived Daily Stage-Specific Irrigation Requirements Using Eto = 4.5 Mm Day⁻¹ and Ea = 90%

Stage	Days	Kc	ETc (mm/day)	GIR (mm/day)	Vd (L/day)	Wp (L/plant/day)	T(min)
Initial	10	0.45	2.025	2.25	225	0.68	21
Development	20	0.70	3.15	3.50	350	1.06	32
Mid-season	30	0.90	4.05	4.50	450	1.36	41
Late season	10	0.75	3.375	3.75	375	1.14	34

The durations in Table 1 refer to each irrigation event, not to a total daily irrigation period. In the present schedule, one irrigation event was programmed per day, so the listed duration is also the total daily pumping duration. If the controller is set for two pulses per day, each pulse should be half the listed duration and the daily total remains the same.

Hydraulic Design Drip Irrigation System

For the peak mid-season water requirement of 450 L/day applied over an irrigation duration of 41 min/day the required system flow was calculated as:

$$Q_{req}, L/h = \frac{Peak\ water\ requirement,}{\frac{L}{day} \times 60} / Duration, min \quad (6)$$

This demand was met using 10 laterals with 33 emitters giving 330 emitters and at a rated discharge of 2 L/h, the design flow became 600 l/h or 1833 L/s which delivered 451 L/day and therefore satisfied the 450 L/day requirement.

Computation of Head Loss in the Pipes and Pumping System Design

Head loss in the lateral, sub-main and mainline pipes was calculated using the simplified Hazen-Williams equation:

$$h_f = 1.21 \times 10^{10} \times \left(Q/C\right)^{1.852} \times D^{-4.87} \times L \quad (7)$$

Where:

H_f = head loss in the lateral, submain, mainline pipe (mm);
Q = flow rate in the lateral, sub-main, mainline pipe L/s);
C = Hazen-Williams roughness coefficient, C= 150 for smooth polyethylene pipe;
D = internal diameter of lateral, sub-main, mainline pipe (mm);
L= length of lateral, sub-main, mainline pipe (m).

For multiple-outlet pipes, the actual and total head losses were calculated using:

$$h_{f(actial)} = h_f \times F \quad (8)$$

$$h_{f(total)} = h_f \times F \times K \quad (9)$$

Where:

F = Christiansen multiple – outlet factor (dimensionless).
K = minor loss factor for emitter barb protrusion (dimensionless taken as K = 1.5 for 16 mm drip tape with inline emitters.

The Christiansen multiple-outlet factor was calculated using:

$$F = \frac{1}{m+1} + \frac{1}{2N} + \frac{\sqrt{m-1}}{6N^2} \quad (10)$$

Where:

m = velocity exponent in the Hazen-Williams equation, m = 1.852;
N = number of outlets along the pipe; Christiansen factor was not applied to the mainline because it does not have multiple outlets. Internal diameters of sub-main and mainline pipes of 20 mm and 25 mm were selected using continuity equation:

$$V = Q/A \quad (11)$$

Where:

$$A = \pi D^2/4 \quad (12)$$

A = cross-sectional area of pipe (m2);
V – velocity of flow in the pipe (m/s);
Q = flow rate (m3/s);
D = internal diameter of pipe (m).

Minor Losses in Fittings

Minor losses through fittings were estimated using velocity head:

$$h_v = v^2/2g \quad (13)$$

$$h_{fittings} = \sum K h_v \quad (14)$$

hv = velocity head;
g – acceleration due to gravity = 9.81m/s2;
$\sum K$ = sum of fitting loss coefficients. For mainline 4.6, sub-main 6.4.

Total Dynamic Head

The total dynamic head was calculated using:

$$TDH = h_{static} + h_{operating} + h_{f,main} + h_{f,sub-main} + h_{f,lat} + h_{,filter} + h_{fittings} \quad (15)$$

Where:

h_{static} = static lift from the water table=6m;
$h_{operating}$ = required operating pressure at emitters =1.5bar = 15.30 m;
$h_{f,\ main}$= mainline friction loss = 0.0755m;
$h_{f,sub-main}$ = sub-main friction loss 0.0907m;
$h_{f,lat}$ = lateral head loss = 0.0107m;
h_{filter} = clean 130-micron disc filter loss = 1.50 m
$h_{fittings}$ = minor loss in fittings = 0.1438m
TDH = 23.12 or 2.27 bar

Pump Selection

The pump duty was therefore: Q ≈ $0.66\ m^3/h$
TDH = 23.1 ≈ $2.27\ bar$
A pump capable of delivering approximately 0.66 m3/h at 25 – 30 m head was selected.

Table 2: Water Pump and Hydraulic Network Specifications

Parameter	Value
Pump rated discharge	**0.66 m³/h (660 L/h)**
Operating head	**23.1 m ≈2.27 bar**
Pump electrical power	**≈83.2 W**
Pump performance characteristics	Duty point **0.66 m³/h at 25–30 m head**; assumed efficiency **0.50**
Number of drip laterals	**10**
Lateral internal diameter	**13.6 mm**
Emitter spacing	**0.3 m**
Nominal emitter discharge	**2.0 L/h**
Operating pressure	**1.5 bar**

Solar Subsystem Design

Assumptions

Pump overall efficiency, η_{pump} = 0.50

Battery efficiency, η_{Batt} = 0.85

Wiring efficiency, η_{wire} = 0.95

Depth of Discharge, DOD =0.50

Days of Autonomy, $N_{autonomy}$ = 1.5 days

Battery nominal voltage, V = 12 V

Peak Sun Hours for Owerri, PSH = 4.5 h/day

PV derating factor = 0.75

Safety factor for PV sizing, SF = 1.5

Mid-season irrigation duration, t = 41 min ≈ 0.6833 h/day

The hydraulic power required by the pump was calculated as:

$$P_h = \rho g Q H \quad (16)$$

Where:

ρ = 1000 kg/m3

g = 9.81 m/s2

Q = 0.66 m3/h = 0.0001833 m3/s

H = TDH 23.12 m

The electrical power drawn by the pump was calculated as:

$$P_e = {P_h}/{\eta_{pump}} \quad (17)$$

Pump energy demand was computed as:

$$E_{pump} = P_e \times t \quad (18)$$

Where:

t = mid-season irrigation duration

Solenoid Valve Energy

Solenoid valve energy was calculated using:

$$E_{valve} = PV_{valve} \times t \ (\frac{Wh}{day}) \quad (19)$$

Where:

Evalve = solenoid valve energy demand

Pvalve = solenoid valve power (8W)

t = daily irrigation duration (h/day)

Controller Energy Demand

Controller energy demand was calculated as:

$$E_{controller} = P_{controller} \times 24 \quad (20)$$

Where:

Pcontroller power (0.8);

24 = hours per day (h/day)

Raw Daily Energy

Raw daily energy was calculated as:

$$E = E_{pump} + E_{valve} + E_{controller} \quad (21)$$

Adjusted Daily Energy

Adjusted daily energy was calculated as:

$$E_{adj} = {E}/{\eta_{Batt} \times \eta_{wire}} \quad (22)$$

Solar Panel Sizing

Sizing of the solar panel was done using the following formulae:

$$PV_{req} = {E_{adj}}/{PSH} \quad (23)$$

$$PV_{rated} = PV_{req} \times SF \quad (24)$$

Calculated PVrated =33.35W, 50 W PV panel was selected.

Average Daily PV Generation

Average daily PV was calculated as:

$$E_{pv} = PV_{rated} \times PSH \times 0.75 \quad (25)$$

Battery Capacity

The battery capacity was computed as:

$$C_{Ah} = {E_{adj} \times N_{autonomy}}/{DOD \times V} \quad (26)$$

Where:

C_{Ah} = battery capacity (Ah);

$N_{autonomy}$ = days of autonomy = 1.5

DOD = depth of discharge = 0.5 (50%) for lead-acid

V = battery nominal voltage = 12V

Selected battery: 12V, 70 Ah lead-acid

Actual Autonomy

The actual autonomy was calculated using:

$$N_{actual} = {C_{Battt} \times V \times DOD}/{E_{adj}} \quad (27)$$

Where:

N_{actual} = actual days of autonomy (days)

C_{Batt} = selected battery capacity (Ah)

Charge Controller Current

The charge controller current was computed as:

$$I_{contr} = I_{sc} \times 1.25 \quad (28)$$

Where:

Icontr = controller rating (A)

Isc = short -circuit current of PV:

$$I_{sc} = {PVwatt}/{V} \quad (29)$$

Where:

1.25 = safety factor for surge

Selected charge controller: 10A, 12V PWM

The solar subsystem characterization is presented in Table 5.

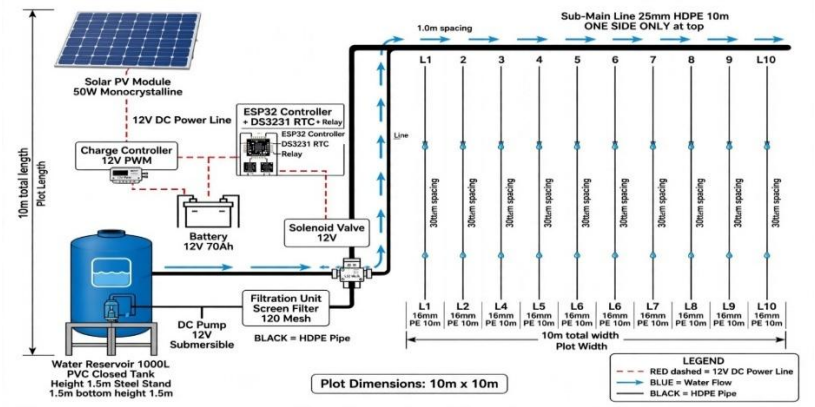


Figure 2: Schematic Layout of the Timer- Controlled Solar-Powered Drip Irrigation System

Controller Design and Programming Logic

This section explains (i) how the ESP32 determines the crop-growth stage and initiates irrigation, (ii) how repeated activation within the same scheduled period is prevented, and (iii) how the system behaves after a power interruption, battery discharge, or clock reset

Controller Hardware and Firmware Architecture

The controller was built around an ESP32-WROOM-32 development board, a DS3231 real-time clock (RTC) module with a CR2032 backup cell, a single-channel opto-isolated relay module driving the DC pump, a 16×2 I²C liquid-crystal display, three momentary push-buttons (SET, UP, DOWN) for local configuration, and a resistor-divider network for battery-voltage sensing. The firmware was written in C++ using the Arduino core and structured as a non-blocking, state-machine loop; no delay () calls were used in the main loop, and the ESP32 hardware watchdog was enabled so that the controller could not hang during a scheduled event.

Timekeeping was delegated entirely to the DS3231, whose temperature-compensated oscillator provides ±2 min year^{-1} accuracy and retains date and time during mains or battery disconnection through its coin cell. The ESP32 therefore never relied on millis() for calendar time. All persistent parameters — transplant date, stage table, programmed durations, last executed event identifier, battery-voltage thresholds and a rolling event log — were stored in non-volatile storage (NVS) using the Preferences library.

Identification of Crop-Growth Sstage

The controller did not infer growth stage from sensors. Instead, it computed days after transplanting (DAT) arithmetically from the calendar date held in the RTC and the transplant date stored in NVS:

text

DAT = (current date) − (transplant date) + 1

The stage was then resolved by a look up against a stage-boundary table:

text

```
const uint8_t NSTAGES = 4;
const uint16_t STAGE_START[NSTAGES] = {1, 11, 31, 61}; // DAT
const uint16_t STAGE END [NSTAGES] = {10, 30, 60, 70}; // DAT
const uint8_t DAILY_MIN [NSTAGES] = {21, 32, 41, 34}; // daily irrigation total
```

A DAT of 1–10 selected the initial stage, 11–30 the development stage, 31–60 the mid-season stage and 61–70 the late-season stage, corresponding to the 10/20/30/10-day partition in Table 3. At DAT > 70 the controller set the pump to permanent OFF and displayed "CROP CYCLE ENDED" until the transplant date was reset, preventing inadvertent irrigation beyond harvest.

Initiation of Irrigation Events

Two irrigation slots were scheduled each day, at 06:00 and 16:30. Because the durations in Table 1 are **daily totals**, each slot delivered half of the daily requirement (Table 4).

Table 3: Daily and Per-Event Irrigation Durations for the Two-Slot Schedule

Stage	DAT	Daily total (min)	06:00 event (min)	16:30 event (min)
Initial	1–10	21	11	10
Development	11–30	32	16	16
Mid-season	31–60	41	21	20
Late season	61–70	34	17	17

The firmware evaluated the schedule once per second in the main loop. An event was initiated only when all four conditions were satisfied:

1. the current hour and minute matched a scheduled slot within a ±1 min matching window;
2. the event identifier for that date and slot had not already been recorded as executed;
3. the battery voltage exceeded the pump-inhibit threshold;

4. the RTC had been validated as holding correct time (Table 5).

When these conditions were met, the controller wrote the event identifier to NVS **before** energising the relay, then asserted the relay and started a non-blocking timer. The relay was de-energised when the accumulated elapsed time reached the stage-specific per-event duration, or when the hardware failsafe limit (1.5 × the programmed duration) was reached, whichever occurred first.

Prevention of Repeated Activation Within the same *Scheduled Period*

Repeated or duplicate activation was prevented by three independent mechanisms, so that no single failure mode could cause over-irrigation.

***Event-identifier Latch*:** Each irrigation opportunity was assigned a unique 32-bit identifier of the form:

text

event ID = (year × 10000 + month × 100 + day) × 10 + slot Number

This identifier was written to NVS and held in RAM as last Event ID *before* the pump was energised. On every loop iteration the controller recomputed the candidate identifier for the current date and slot; if it equalled last Event ID, the event was skipped. Because the identifier includes the calendar date, the latch cleared automatically at midnight without any explicit reset, and it remained effective across reboots because it was stored in NVS.

Narrow Matching Window with Slot Expiry: The slot-matching window was limited to ±1 min around the nominal time. If the controller was not running during that window — for example, because of a power failure — the slot expired and was not retroactively executed. The pump could therefore never be triggered by a time match that persisted for a long period.

Minimum off-time Lockout: A lockout timer enforced a minimum interval of 120 min between consecutive pump events and a minimum pump-off period of 5 min after any event terminated. This prevented relay chatter, rapid re-triggering from repeated RTC alarm flags, and repeated activation caused by transient time corrections.

In addition, the RTC alarm flags were cleared after each read, so that a latched alarm could not re-trigger the pump on the following loop iteration.

Behaviour After Power Interruption, Battery Discharge or Clock Reset

The controller was designed so that each fault condition produced a defined and safe response rather than an uncontrolled or duplicated irrigation (Table 5).

Power Interruption during an Event: On boot, the firmware first read the pump state flag from NVS. The relay was unconditionally driven LOW before any other initialisation, so a pump that had been running when power was lost could not restart in an uncontrolled manner. The controller then compared the stored event start timestamp with the current RTC time. If the interruption had occurred within a 30 min grace period and less than the full programmed duration had elapsed, the remaining time was completed; otherwise the partially completed event was logged as "interrupted" and abandoned, and normal scheduling resumed at the next slot. This avoided applying a full irrigation at an inappropriate time of day after an extended outage.

Battery Discharge: Battery voltage was sampled every 30 s through the resistor divider and a running median filter. The pump was inhibited when voltage fell below 11.5 V (12 V lead-acid equivalent), the display showed "LOW BATTERY", and the affected event was logged as "skipped – low battery" rather than being queued for later execution. Automatic irrigation resumed only after the battery had recovered above 12.2 V, providing hysteresis against repeated inhibit/re-enable cycling. Voltage thresholds were stored in NVS and could be reconfigured from the keypad.

Clock Reset or Loss of RTC Time: The DS3231 oscillator-stop flag (OSF, status register 0x0F) was read at every boot. If the flag was set, indicating that RTC time had been lost, the firmware cleared the flag, set clock Valid = false, and entered a safe mode in which automatic scheduled irrigation was disabled and the display prompted for manual time entry. Normal automatic operation resumed only after the date and time had been re-entered and confirmed. The transplant date and stage table were retained in NVS throughout, so re-establishing the clock did not require reconfiguration of the crop schedule. Manual irrigation remained available in safe mode, but was limited to a single maximum-duration pulse to prevent an unattended continuous run.

Table 4: Fault Response Matrix

Fault condition	Detection method	Controller response	Irrigation outcome
Power loss during event	NVS pump-state flag + stored start timestamp	Relay forced OFF at boot; elapsed time recomputed from RTC	Remaining time completed if within 30 min grace period, otherwise logged as interrupted and abandoned
Battery below threshold	ADC divider, 30 s sampling	Pump inhibited; "LOW BATTERY" displayed; event logged as skipped	Event not executed and not queued
Battery recovery	ADC divider, hysteresis at 12.2 V	Automatic scheduling re-enabled	Normal schedule resumes at next slot
RTC time lost	DS3231 OSF flag at boot	Clock Valid = false; automatic mode blocked; manual time-entry prompt	No automatic irrigation until clock revalidated
Duplicate trigger	Event-ID latch in NVS; ±1 min window; 120 min lockout	Event skipped	No duplicate event
Firmware hang	ESP32 hardware watchdog	Forced reset; relay default state OFF	Event handled as a power-interruption case on reboot

Testing and Performance Evaluation

Emitter Discharge

The ASAE method was used. Forty emitters were selected- 4 per lateral at head, 1/3, 2/3 and tail end. Water from each emitter was collected into catch cans under regulated pressure of 1.5bar for 15 minutes using a stopwatch. The volumes of water from each emitter were collected three times and recorded.

Using the volumetric method, emitter discharge for each run was determined as follows:

Measured volume was converted to L/h using:

$$q = {Volume\ (ml) \times 60}\Big/{time\ (\text{min}) \times 1000} \quad (30)$$

The average emitter discharge was determined using:

$$q_a = {1}/{n} \sum_{i=1}^{n} q_i \quad (31)$$

Where:

q_a = average emitter discharge rate (L/h);

q_i = emitter flow rate (L/h);

n = total number of emitters

In all, 40 emitters had their average discharges measured and recorded: 1.95, 2.05, 1.90, 2.02, 1.92. 2.00, 1.88, 2.01, 1.90, 1.98, 1.85, 2.00,1.88, 1.95, 1.82, 1.98, 1.85, 1.92, 1.80, 1.95, 1.85, 1.90, 1.80, 1.93, 1.82, 1.88, 1.77, 1.90, 1.80, 1.85, 1.75, 1.88, 1.98, 1.95, 1.85, 2.01, 1.98, 1.88, 1.92, 1.82 L /h

Coefficient of Variation

Coefficient of variation was calculated as per ASAE EP 458:

$$CV = {s_d}/{q_a} \times 100 \quad (32)$$

Where:

CV= coefficient of variation (%);

s_d= standard deviation of emitter discharge rates in the sample (L/h);

q_a = average discharge of all sampled 40 emitters (L/h);

Coefficient of Uniformity

The uniformity coefficient for emitter flow variation was calculated according to Christiansen (1942) as:

$$CU = \left(1 - \frac{\sum |x|}{m \times n}\right) \times 100 \quad (33)$$

Where:

CU = uniformity coefficient (%);

x = absolute deviation of the individual observation from the mean discharge (l/h);

m = mean of all observations (l/h);

n = number of observations.

Emission Uniformity

Emission uniformity was calculated using the Keller and Blaisner method:

$$EU = {q_n}/{q_a} \times 100 \quad (34)$$

Where:

EU = emission uniformity

q_n = average discharge of lowest ¼ of emitters (L/h)

q_a = average discharge of all sampled emitters (L/h)

$$FV = {q_{max} - q_{min}}/{q_{max}} \times 100$$

Where:

FV = flow variation (%)

q_{max} = maximum discharge (L/h)

q_{min} = minimum discharge (L/h)

Timer Error

The system was powered with a fully charged 12 V battery, and the DS3231 RTC was synchronized to the compile time. Daily irrigation was programmed to trigger at 06:00. For each growth stage, three replicate measurements were taken from three independent controller cycles / three repeated actuations within one session. The DS3231 internal timestamp shown on the serial monitor was recorded as the controller-command time. Actual valve opening and closing were determined by direct observation of the solenoid valve/water outlet and timed with an external digital stopwatch (0.01 s resolution) under field conditions at the FECOLART Students Research and Demonstration Farm. The stopwatch values were used to assess physical valve response; the DS3231 timestamp alone was not assumed to represent the physical response.

The timer error was then estimated using standard formulae specified by ASAE S526.2:

Absolute Error (min)

$$\text{Error (min)} = T_m - T_p \quad (35)$$

Percentage Timer Error (%)

$$\text{Timer Error (\%)} = {T_m - T_p}\Big/{T_p} \times 100 \quad (36)$$

Timer Accuracy (%)

$$= 100 - \left({T_m - T_p \times 100}\Big/{T_p}\right) \quad (37)$$

To describe the overall performance of the system, the following statistical measures were computed:

Mean Error (%):

$$E = {\sum E_i}/{n} \quad (38)$$

Standard Deviation:

$$SD = \sqrt{{\sum (E_i - E_m)^2}/{n-1}} \quad (39)$$

Root Mean Square Error:

$$RMSE = \sqrt{{\sum \left(T_m - T_p\right)^2}/{n}} \quad (40)$$

Where:

Ei = individual timer error (%)

N = number of observations (12 = 4 stages × 3 replicates)

Acceptance Criteria used according to ASAE and irrigation automation:

Acceptable:$|Timer\ Error| \leq 5\%$

Excellent:$|Timer\ Error| \leq 2\%$

Fail: $|Timer\ Error| > 5\%$

Data Analysis

Data were subjected to One-Way Analysis of Variance (ANOVA) using SPSS v27 / Excel Data Analysis Toolpak at 5% level of significance ($p<0.05$). Mean separation was done using Duncan's Multiple Range Test (DMRT) to compare timer errors across growth stages. This method directly estimates timer drift, relay switching lag, and RTC accuracy for offline operation without internet/WiFi.

RESULTS AND DISCUSSION

Operational Performance of the Power Subsystem

The power subsystem (Table 5) performs adequately under nominal conditions because the 50 W PV module exceeds the calculated requirement of about 33.35 W and is expected to generate about 168.75 Wh/day against an adjusted daily demand of about 100.9 Wh/day.

Table 5: Power Subsystem Characterisation

Parameter	Value
PV module rated power	50 W (calculated requirement ≈33.35 W)
Battery capacity	12 V, 70 Ah lead-acid
Actual autonomy at 50% DoD	≈4.16 days
Pump hydraulic power requirement	≈41.6 W
Pump electrical power requirement	≈83.2 W at pump efficiency 0.50
Charge controller specifications	10 A, 12 V PWM (required current ≈5.21 A)
Expected daily energy consumption	Raw ≈81.5 Wh/day; adjusted ≈100.9 Wh/day
Expected daily PV generation	≈168.75 Wh/day
Operation under reduced solar irradiance	PV output falls proportionally with peak sun hours; PV meets adjusted daily demand at ≈2.69 h/day peak sun; below this, the battery supplies the deficit

This provides a nominal surplus of about 67.85 Wh/day, or a generation-to-demand ratio of roughly 1.67, which should support pump operation and battery charging when solar irradiance is sufficient. The 10 A, 12 V PWM charge controller is also adequate because the required current is only about 5.21 A.

The 12 V, 70 Ah lead-acid battery has about 840 Wh of nominal capacity and about 420 Wh usable at 50% depth of discharge, giving an estimated autonomy of about 4.16 days at the adjusted daily demand. The pump discharge rate of about 6.93 A corresponds to roughly 0.099C for this battery, which is a reasonable operating rate for a lead-acid battery. However, this autonomy is theoretical because temperature, voltage drop, and charging efficiency can reduce usable capacity, and recharge from 50% depth of discharge using only the nominal PV surplus would take about 6.2 days before charging losses are considered.

The pump's electrical power requirement is about 83.2 W at 50% pump efficiency, against a hydraulic power requirement of about 41.6 W, so roughly half of the electrical input is lost in the pump and motor system. At 12 V this gives a pump current of about 6.93 A, consistent with the reported value. The raw daily energy demand of about 81.5 Wh/day implies about 0.98 hours of pump runtime per day, while the adjusted demand of about 100.9 Wh/day implies about 1.21 hours per day; at the rated discharge of 660 L/h, this corresponds to roughly 650–800 L/day depending on the demand basis used. Under reduced solar irradiance, PV output falls proportionally with peak sun hours, and the system is reported to meet adjusted daily demand at about 2.69 peak-sun hours per day, below which the battery supplies the deficit. This threshold is consistent with an assumed PV system derating of about 75%; without derating, the equivalent threshold would be about 2.02 peak-sun hours per day. Overall, the power subsystem is appropriately sized for nominal operation with a useful PV surplus and about four days of battery autonomy at 50% depth of discharge, but its performance is sensitive to actual irradiance, pump runtime, battery efficiency, and PV derating.

Hydraulic Performance of Drip Irrigation System

System's Hydraulic Parameters and their Ratings

Table 6 shows the hydraulic performance rating of the drip system in which both the Coefficient of Uniformity (CU) at 96.74% and the Emission Uniformity (EU) at 95% exceed the 90% threshold for an "Excellent" rating, indicating that the system delivers water very evenly across the field, which is the primary goal of drip irrigation design.

Table 6: Values and Ratings of the Hydraulic Parameters of the Timer-Controlled Solar- Powered Drip Irrigation System

Parameter	Calculated Value	Rating Standard (ASAE EP458)	Performance Rating
CU	96.74%	> 90% is Excellent (ASAE EP458, 1999 ed.)	Excellent
EU	95.00%	> 90% is Excellent (ASAE/ASABE EP458)	Excellent
CV	3.96%	< 10% is Excellent (Standard ASAE criteria; 2002 ed. also rates <5% as "Perfect")	Excellent
FV	14.63%	10%–15% is Fair (ASAE EP458, 2005d ed.)	Fair

The low CV (3.96%) confirms that the individual emitters are performing very consistently. The FV value of 14.63% ("Fair") introduces a note of nuance. While FV is related to uniformity, it specifically captures the extreme spread between the highest and lowest emitter discharges. A "Fair" FV rating suggests that, despite the excellent average performance, there is a more noticeable difference between the best- and worst-performing emitters than would be present in an "Excellent" or "Very Good" system. This could stem from minor pressure variations along the laterals, slight differences in emitter manufacturing, or the very early stages of partial clogging in some emitters.

Overall, the Table Presents Strong Evidence that the System Performs well

Average Discharge Rates of Emitters from Sampled Laterals

The emitter flow variation across the 40 sampled emitters shows a mean discharge of **1.903 L/h** L/h compared to the rated discharge of 2.00 L/h, representing a deviation of only 4.85% is presented in Figure 3.

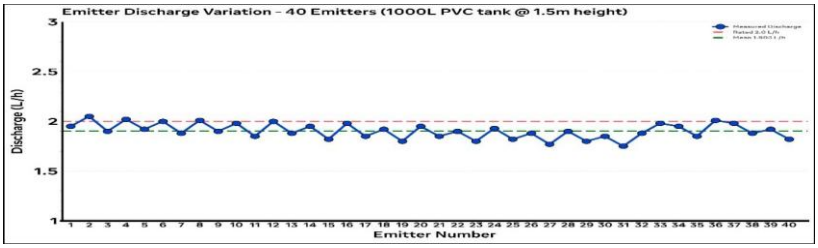


Figure 3: Variation of Emitter Discharge Rates Across Drip Lines

The measured flow rates range from approximately 1.82 L/h to 2.05 L/h, giving a narrow total spread of about 0.23 L/h around the rated value. Most emitters cluster closely around the rated discharge, with the highest values near emitters 2 and 8 at about 2.05 L/h and the lowest values near emitters 15 and 11 at about 1.82 L/h and 1.85 L/h, respectively. The variation across emitter numbers appears small and random, with no clear increasing or decreasing trend, which indicates that the emitters are operating very close to their rated discharge. Because the mean line lies slightly below the rated line, the system as a whole is performing slightly below the 2.00 L/h rating while still remaining within a small and generally acceptable range. Overall, the graph supports the conclusion that emitter discharge is reasonably uniform and close to the rated value, with only minor and random deviations.

Operational Flow Chart of Timer-Based Solar Powered Drip Irrigation System

Figure 4 outlines the microcontroller logic for a timer-based drip irrigation system designed for a 70-day cucumber crop cycle. It uses a Real-Time Clock (RTC DS3231) to automate watering twice a day based on the plant's growth stage.

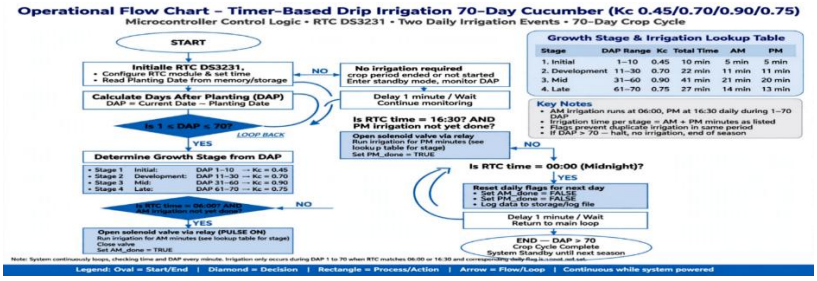


Figure 4: Operational Flow Chart of Timer-Based Solar Powered Drip Irrigation System

The System Operates through the Following Sequence

1. Initialization & Growth Tracking: The system starts by setting the RTC time and reading the planting date. It calculates the Days After Planting (DAP) by subtracting the planting date from the current date. If DAP is not between 1 and 70, the system enters a standby mode (no irrigation). If it is within 1–70 days, it determines the current growth stage (Initial, Development, Mid, or Late).
2. Irrigation Scheduling: Based on the growth stage (which determines the crop coefficient, Kc), the system looks up the required watering duration for the morning (AM) and evening (PM). If the time is 06:00 and the AM flag isn't set, it opens the solenoid valve for the designated AM duration and sets the AM_done flag to true. Similarly, at 16:30, if the PM flag isn't set, it opens the valve for the PM duration and sets the PM done flag.
3. Daily Reset & Looping: At midnight (00:00), the system resets the AM and PM flags to FALSE (preparing for the next day's irrigation) and logs the data. The system then delays for 1 minute and loops back to the start to continuously monitor the time and DAP, ensuring irrigation only happens once per scheduled period.

The total watering duration varies by stage: Stage 1 (Initial) requires 10 mins, Stage 2 (Development) 22 mins, Stage 3 (Mid-season) 41 mins (peak water need), and Stage 4 (Late-season) 27 mins.

Developed Growth Stage Schedule for Cucumber

Figure 5 presents a comprehensive growth stage irrigation schedule, detailing the required water volumes and application timings.

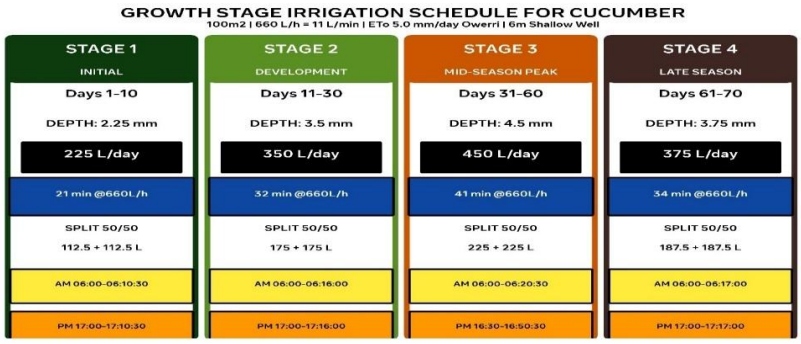


Figure 5: Growth Stage Irrigation Schedule

The cucumber plant requires the most water during Stage 3 (Days 31–60), needing 450 liters daily. The schedule mandates a strict 50/50 split every day—an agricultural best practice where morning watering reduces evaporation and evening watering ensures the plant has moisture during the night. The system's flow rate remains constant at 660 L/h throughout all stages; thus, the only variable that changes is the pump's run duration. The water volume follows the biological growth curve: starting at 225 liters, ramping up to 350 liters, peaking at 450 liters, and tapering off to 375 liters as the plant matures.

Comparison of Programmed and Measured Times

Figure 6 illustrates the comparison between programmed and measured valve-open times across the four growth stages.

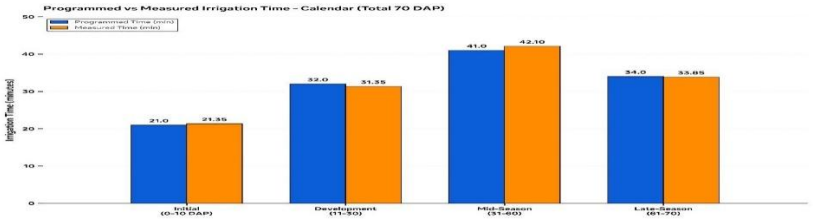


Figure 6: Comparison of Programmed Vs Measured Solenoid Valve Open Times Across Growth Stages

The programmed durations of 21, 32, 41, and 34 minutes for the initial, development, mid-season, and late-season stages closely matched the measured values of 21.35, 31.7, 42.1, and 33.85 minutes, respectively. The minor deviations (+0.35, -0.30, +1.10, and -0.15 minutes) are attributed to relay switching lag and solenoid inertia. The near-overlapping of both lines confirms minimal drift of the DS3231 RTC.

Percentage Timer Error and Accuracy Across Growth Stages

Figure 7 illustrates the percentage timer error by growth stage.

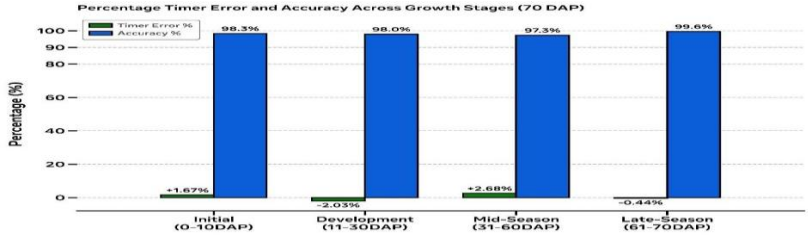


Figure 7: Percentage Timer Error and Accuracy Across Growth Stages

The recorded errors were +1.67%, -0.94%, +2.68%, and -0.44% for the initial, development, mid-season, and late-season stages, respectively. All errors fall within the ±5% acceptable limit for irrigation automation. The observed maximum error of +2.68% occurred at the mid-season stage (41 min), likely due to 12V relay switching lag and slight voltage drops during longer operations. Overall, the system achieved a mean error of +0.74% and a mean accuracy of 98.57%, demonstrating reliable offline performance.

Statistical Analysis of Timer Error

Table 7 shows ANOVA for timer error %) across growth stages for 70 DAP calendar.

Table 7: ANOVA for Timer Error (%) Across Growth Stages

Source of Variation	DF	SS	MS	Fcal	P-value	Inference
Between Group Stages	3	26.1512	8.7171	80.86	0.0000025	Highly Significant
Within Groups (Error)	8	0.8620	0.1078			
Total	11	27.0132				

Significant at p < 0.001

Timer error differed significantly among growth stages ($F = 80.86$, $p < 0.001$), indicating systematic variation in timer error with programmed irrigation duration/growth stage. The largest positive error (+2.68%) occurred at the mid-season stage (41 min), consistent with cumulative relay lag and solenoid-valve inertia during longer actuations. The magnitude and uncertainty of the errors were then assessed against the ±5% ASAE acceptance limit: mean error = +0.74%, SD = 1.72%, 95% CI = −1.99% to +3.47%, MAE = 1.43%, RMSE = 1.66%, and maximum absolute error = 2.68%. All observed errors remained within the ±5% limit; therefore, relative to this predefined acceptance criterion, the ESP32-DS3231 system showed acceptable timing accuracy over the 70-day cucumber cycle. The fitted model explained a high proportion of the variance in timer error ($R^2 = 0.968$), but this value describes the proportion of systematic variation in timer error associated with growth stage/programmed duration; it is not, by itself, a measure of accuracy. Accuracy is supported by the small, bounded errors relative to the ±5% limit, whereas repeatability/precision is supported by the replicate variability reported above.

Discussion

The results in Table 6 position the timer-based solar-powered drip irrigation system as a high-performing and precise solution for cucumber cultivation, aligning closely with international standards and the broader body of irrigation

research. The hydraulic parameters in Table 6 indicate that the system delivers water with exceptional uniformity and consistency, surpassing many conventional benchmarks. The recorded coefficient of uniformity (CU) of 96.74% and emission uniformity (EU) of 95% fall squarely into the "Excellent" category according to ASAE Standards EP 458, which classifies CU and EU values above 90% as excellent (ASABE, 1999). These figures are notably higher than those reported in comparable studies on automatic drip systems. For instance, Sewilam et al. (2025) evaluated automatic and manual drip irrigation control systems and reported emission uniformity values in the "Good" range (approximately 80–86%), with coefficient of uniformity values around 87%, indicating that the present system achieves a superior level of emission consistency. Similarly, research on solar-powered drip irrigation for greenhouse cucumbers found uniformity values that were high but did not reach the exceptional levels achieved here (Okasha, 2016). The system's performance is indicative of a well-designed hydraulic network, likely utilizing high-quality, pressure-compensating emitters. Furthermore, the coefficient of variation (CV) of 3.96% is well below the 10% threshold considered "Excellent" for emitter consistency. While the flow variation (FV) of 14.63% is rated as "Fair" (10%–15% is Fair (ASAE EP458, 2005d ed.)) This slight flow variation is common in field conditions and is generally attributed to friction losses and minor pressure fluctuations along the lateral line. These observations align with Barroso et al. (2022), who quantified mean absolute flow errors of 5.1 L/min for open-loop timer control and 4.8 L/min for closed-loop control under load, indicating that even controlled drip systems exhibit measurable flow deviations under field load. In addition, Lozano et al. (2020) demonstrated that short pulses (<21 min) can reduce distribution uniformity because of filling and emptying phases; the present system's high CU and EU nevertheless indicate that its hydraulic design and pressure-compensating emitters offset such pulse-related risks across the stage-specific irrigation durations. Overall, the combination of a very low CV and high CU/EU confirms that the system minimizes both under- and over-watering, which is critical for uniform crop growth and resource efficiency.

The timing control results from the ANOVA (Table 7) further validate the system's reliability, demonstrating that the ESP32-DS3231 controller maintains high precision even as irrigation demands change across growth stages. The ANOVA revealed a highly significant difference in timer error across growth stages ($F = 80.86$, $p < 0.001$), with an R^2 of 0.968, meaning 96.8% of the variation in timer error is explained by the programmed duration. This indicates that the system's timing behavior is highly predictable and stage-dependent. The highest positive error (+2.68%) occurred at the mid-season stage with the longest 41-minute irrigation duration, attributed to cumulative relay lag and solenoid valve inertia. This is consistent with electromechanical realities; longer operational cycles naturally accumulate more actuation delay. Crucially, all timer errors remained within the ±5% limit stipulated by ASAE standards, confirming that the system is more than sufficiently accurate for practical irrigation scheduling (ASABE, 1999). This level of precision aligns with findings from other research on ESP32/DS3231-based controllers. For example, Nurohmah et al. (2026) reported 100% schedule execution success and 100% relay–pump state reliability for a comparable ESP32–DS3231 hydroponic irrigation prototype, with the RTC showing a recorded 0-s difference from the daily reference time over five observation days. While a study on a timer-based control system for greenhouse tomatoes reported a cumulative water application error of 7.01% (Kaunkid, 2019), the current system's maximum error of +2.68% represents a marked improvement in timing precision. The present result also contrasts with broader timer-control literature. Kim et al. (2015) showed that keep-pause logic is strongly affected by sunlight, causing timing drift; in the present ESP32–DS3231 system, RTC-based scheduling avoids sunlight-dependent keep-pause behavior. Swanson and Fipps (2009) at Texas A&M found that timer-based controllers applied 0.33 to 2.5 times the recommended water, with manual timers applying twice as much water as needed, attributed to improper ET values and high crop coefficients. These findings underscore that timer-based irrigation can be accurate only when scheduling is matched to crop water demand; here, stage-specific programmed volumes (e.g., 450 L/day at mid-season peak) and errors below ±3% reduce the risk of systematic over- or under-application. Barroso et al. (2022) further showed that flow errors can persist under both open- and closed-loop timer control (5.1 and 4.8 L/min, respectively), reinforcing the importance of combining precise timing with hydraulic uniformity. This confirms that the ESP32–DS3231 combination provides robust timing control, ensuring that the carefully calculated water volumes for each growth stage are applied accurately.

In summary, the results demonstrate that the system achieves excellent hydraulic uniformity (CU > 96%, EU = 95%) and highly precise timing control (errors < ±3%, well within ASAE limits). These findings are consistent with, and in many cases exceed, the performance reported in the literature for similar solar-powered and timer-based drip irrigation systems, including timer-control studies reporting pulse-related uniformity losses (Lozano et al., 2020), flow errors under timer control (Barroso et al., 2022), sunlight-induced timing drift in keep-pause logic (Kim et al., 2015), and over-application by timer-based controllers (Swanson and Fipps, 2009), confirming its suitability for efficient cucumber production.

CONCLUSION

A timer-controlled solar-powered drip irrigation system incorporating an ESP32 microcontroller and DS3231 real-time clock was developed and evaluated for irrigation scheduling across a 70-day cucumber growth cycle. The prototype achieved a coefficient of uniformity of 96.74%, emission uniformity of 95% and coefficient of variation of 3.96%, indicating favourable hydraulic performance under the investigated conditions. The reported flow variation was 14.63%, while measured timer errors ranged from −0.94% to +2.68% across the four programmed growth stages. Analysis of variance indicated significant differences in timing errors among the stages. These findings suggest that the developed system can provide relatively uniform emitter discharge and maintain programmed irrigation durations with limited timing deviations. However, the study did not establish long-term solar-power reliability, actual irrigation-water savings or improvements in cucumber growth and yield. Further investigations incorporating complete solar-energy performance measurements, extended field trials, crop-water balance assessment and economic evaluation are recommended before the system is proposed for wider smallholder-farming applications.

REFERENCES

Adeyolanu, D. T., & Okelola, O. E. (2024). Irrigation water management and food security in Nigeria. *African Journal of Agriculture and Food Science, 7*(4), 117–132. https://doi.org/10.52589/AJAFS-PFPU1QN7

Amaechina, E. C., & Eboh, E. C. (2013). *Towards commercialization of irrigated agriculture in Nigeria: Lessons from the Lower Anambra Irrigation Project South-East Nigeria* [Conference paper]. Fourth International Conference of the African Association of Agricultural Economists (AAAE), Hammamet, Tunisia. https://doi.org/10.22004/ag.econ.160296

American Society of Agricultural and Biological Engineers. (1999). *Field evaluation of microirrigation systems* (ASAE Standards EP458). ASABE.

American Society of Agricultural Engineers. (2002). *ASAE standards: Standards, engineering practices and data adopted by the American Society of Agricultural Engineers* (Vol. 2002). American Society of Agricultural Engineers.

American Society of Agricultural and Biological Engineers. (2005). *ASAE EP458: Field evaluation of microirrigation systems*. ASABE.

Barroso, F. S. M., Inácio, M. J., & Oliveira, F. G. (2022). Embedded fuzzy controller for application in irrigation systems. *Engenharia Agrícola*, *42*, e20210138. https://doi.org/10.1590/1809-4430-eng.agric.v42nepe20210138/2022

Berdiyeva, D., Otajonov, I., Kiryigitova, S., Sobirova, M., & Sherkuziyeva, G. (2025). Impact of heavy metals (copper, cadmium, mercury, and lead) on the fertility, microbiological activity, and crop productivity of irrigated meadow soils: A literature review from an ecological and food security perspective. *Journal of Carcinogenesis*, *24*(8s), 352–359. https://doi.org/10.64149/J.Carcinog.24.8s.352-359

Bichi, M., & Abdulyakin, M. (2025). Comprehensive analysis of soil physical properties and their relationships: Recommendations for optimized irrigation strategies. *CIGR Journal*.

Erdem, Y., Arin, L., Erdem, T., Polat, S., Deveci, M., Okursoy, H., & Gültaş, H. T. (2010). Crop water stress index for assessing irrigation scheduling of drip irrigated broccoli (*Brassica oleracea* L. var. *italica*). *Agricultural Water Management*, *98*(1), 148–156. https://doi.org/10.1016/j.agwat.2010.08.013

Food and Agriculture Organization of the United Nations. (2022). *RuLIS – Rural Livelihoods Information System* [Data set]. https://www.fao.org/in-action/rural-livelihoods-dataset-rulis/data-application/data/by-indicator/en

Igbojionu, D. O., Ekejiuba, V. N., Igbojionu, J. N., Ezema, P. C., Sampson, H., & Chiemeka, C. I. (2026). Optimizing irrigation regimes and intervals for improved water productivity and yield of cucumber (*Cucumis sativus*) in a tropical agroecological zone. *FUDMA Journal of Sciences*. https://doi.org/10.33003/fjs-2026-1016-3821

International Renewable Energy Agency. (2023). *Off-grid renewable energy statistics 2023*. https://www.irena.org/publications/2023/Dec/Off-grid-renewable-energy-statistics-2023

Kaunkid, S. (2019). Irrigation control system for drip irrigated tomato in greenhouse using timer-based control method and crop water requirement. *Warasan Witthayasat Lae Theknoloyi Mahawitthayalai Mahasarakham*, *38*(2), 164–172.

Kim, H. J., Lee, D. H., Ahn, S. W., Kim, W. K., Hur, S. O., Choi, J. Y., & Chung, S. O. (2015). Design and testing of an autonomous irrigation controller for precision water management of greenhouse crops. *Engineering in Agriculture, Environment and Food*, *8*(4), 228–234. https://doi.org/10.1016/j.eaef.2015.03.001

Kuzyakov, Y., Horwath, W. R., Dorodnikov, M., & Blagodatskaya, E. (2019). Review and synthesis of the effects of elevated atmospheric CO_2 on soil processes: No changes in pools, but increased fluxes and accelerated cycles. *Soil Biology and Biochemistry*, *128*, 1–14. https://doi.org/10.1016/j.soilbio.2018.10.005

Li, R., Han, Q., Dong, C., Nan, X., Li, H., Sun, H., Li, H., Li, P., & Hu, Y. (2023). Effect and mechanism of micro-nano aeration treatment on a drip irrigation emitter based on groundwater. *Agriculture*, *13*(11), 2059. https://doi.org/10.3390/agriculture13112059

Lozano, D., Ruiz, N., Baeza, R., Contreras, J. I., & Gavilán, P. (2020). Effect of pulse drip irrigation duration on water distribution uniformity. *Water*, *12*(8), 2276. https://doi.org/10.3390/w12082276

Nigerian Meteorological Agency. (2023). *2023 Seasonal Climate Prediction (SCP)*. http://ngfrepository.org.ng:8080/jspui/handle/123456789/5461

Nurohmah, H., Ali, M., & Prianandа, C. W. (2026). RTC-scheduled ESP32 IoT prototype for automated hydroponic nutrient irrigation. *Journal of Robotics, Embedded Systems, and Data Analytics*, *3*(2). https://doi.org/10.66314/joresd.v3i2.694

Okasha, A. (2016). Maximizing irrigation water use efficiency and utilization of solar energy with drip irrigation systems for cucumber production inside greenhouse. *Journal of the Advances in Agricultural Researches*, *21*(3), 454–472.

Olayide, O. E., Tetteh, I. K., & Popoola, L. (2016). Differential impacts of rainfall and irrigation on agricultural production in Nigeria: Any lessons for climate-smart agriculture? *Agricultural Water Management*, *178*, 30–36. https://doi.org/10.1016/j.agwat.2016.08.034

Pavithra, N., Kasara, A. A., Darshini, M., Chethana, G., & Shiny, L. (2018). *International Journal of Computer Engineering and Applications*, *12*, 1–5.

Sewilam, M. R., Elmetwalli, A. M. H., Mohammed, S., & Amer, M. M. (2025). Comparative evaluation of automatic and manual drip irrigation control systems under variable valve opening levels. *Journal of Sustainable Agricultural and Environmental Sciences*, *4*(1), 1–12.

Swanson, C., & Fipps, G. (2009). *Evaluation of smart irrigation controllers: Initial bench testing results*. Texas Water Resources Institute, Texas A&M University System.

van Opstal, J., & Food and Agriculture Organization of the United Nations. (2021). *Guidance on realizing real water savings with crop water productivity interventions: An action framework for agriculture and food security* (FAO Water Reports No. 46). FAO. https://katalog.ub.uni-leipzig.de/Record/3-9789251341360

©2026 This is an Open Access article distributed under the terms of the Creative Commons Attribution 4.0 International license viewed via https://creativecommons.org/licenses/by/4.0/ which permits unrestricted use, distribution, and reproduction in any medium, provided the original work is cited appropriately.